



# A Proposed Optimization Model for Water Quality Prediction in Internet of Things Environment

**Gopal Chaudhary, Puneet Singh Lamba, Deepali Virmani**

VIPS-TC, School of Engineering & Technology, New Delhi, India

Emails: Gopal.chaudhary88@gmail.com; puneet.lamba@vips.edu; deepalivirmani@gmail.com

## Abstract

The application of industrialization and urbanization strategies results in the proliferation of waste products in water resources which is a serious public challenge. They have resulted in calls for advanced technologies of water quality mitigation and monitoring, as emphasized in the sustainable development objectives. Now, environmental engineering researcher is looking for a more complex process of implementing practical assessments and of monitoring the quality of ground and surface water that is quantifiable to human beings over different locations. Many current techniques use the Internet of Things (IoT) for water quality assessment and monitoring. This paper explores the proposal of African Buffalo Optimization with Deep Belief Network for Water Quality Prediction (ABODBN-WQPR) model in an IoT environment. The presented proposed model majorly concentrates on the identification of water quality.

**Keywords:** Internet of Things; Water quality prediction; Deep learning; Artificial buffalo optimization; Deep belief network; Hyperparameter optimizer

## 1. Introduction

As a significant part of the natural atmosphere, the water atmosphere serves a fundamental part of human existence. With the quick improvement of industry, the release of modern wastewater has expanded step by step, prompting the decay of water climate, and water climate insurance is confronting extreme difficulties [1, 2]. Precise water quality (WQ) expectation becomes the reason for water climate assurance. The monitoring focuses are furnished with different WQ Internet of Things (IoT) gadgets to assemble water natural IoT framework that could gather WQ data progressively, making the expectation of exact WQ conceivable. Customary techniques for WQ expectation are grouped into regression analysis, dark system, and NN [3]. The WQ forecast strategy in view of regression analysis was gotten from numerical measurements. It decides the connection between the reliant variable and free factor through the analysis of measurable data, and works out the relationship co-efficient via a specific calculation, in this way building a regression condition to foresee WQ data [4].

The improvement of AI, remote sensing (RS), distributed computing, IoT, enormous data and gives new open doors and ways to deal with the advancement and utilization of water climate monitoring innovation [5]. Depending on various types of hydrological and monitoring ships, WQ automated monitoring stations, wireless sensor networks (WSNs), brilliant monitoring systems and RS monitoring systems, and high-level underwater bionic robots for water climate assurance were implicit in urban communities and provinces in China. Based on the historic data gathered by the brilliant WQ monitoring systems, a WQ expectation method could lay out a comparing planning connection among multi-monitoring data and progressions of WQ boundaries and could foresee variations in the state of WQ in specific periods [6].

Lately, the foundation of solid WQ expectation methods has turned out to be the study areas of interest in the domain of water ecological science. Nonetheless, by the large-scale utilization of the brilliant

WQ monitoring system [7], albeit the inadequacies of the customary assortment technique are settled, a large measure of the enormous dataset is delivered. Furthermore, the water climate is impacted by various components and has solid nonlinear qualities. Nonetheless, the conventional WQ expectation model can't exhaustively think about the impact of physics, biology, chemistry, hydraulics, and meteorology factors [8]. As of now, authors for the most part center around working on the pertinence and dependability of WQ expectation methods and have presented various new advancements, like stochastic mathematics, fuzzy mathematics, ANN, 3S innovation, and so on, to further develop WQ forecast methods and advance the extent of uses. WQ alludes to the physical, synthetic, and organic attributes of water [9]. Evaluation and monitoring of WQ are fundamental since it assists in conveniently distinguishing proof of expected ecological issues because of the multiplication of contaminations (from anthropogenic exercises) [10]. Normally, it is performed in the short and long haul. Monitoring and evaluation are additionally key with the goal that potential guideline offenders can be distinguished.

Zou et al. [11] present a technique for WQ prediction (WQP) dependent upon the multiple time scale bi-directional LSTM (BiLSTM) network. This technique can enhance data volume and data integrity with data pre-processing. Then, the process input data forward as well as backward and assume the dependency at several time scales. Moreover, it can utilize the Box–Behnken experimental design approach for adjusting hyperparameters during the procedure of modeling. Yan et al. [12] examine a novel comprehensive DL-WQP technique. Primarily, the WQ data is the cleaning and pre-treating with isolation forest, Lagrange interpolation approach, sliding window average, and PCA. Afterward, one-dimensional residual CNNs (1-DRCNN) and BiGRU were utilized for extracting the potential local feature amongst WQ parameters and combining data before and after time series.

In [13], advanced AI techniques were established for predicting WQI and WQ classification (WQC). In order to WQI prediction, ANN techniques such as nonlinear autoregressive neural network (NARNET) and LSTM, DL techniques are established. Besides, three ML approaches SVM, KNN, and NB are utilized for WQC forecast. In [14], two new hybrid DT-based ML approaches were presented for obtaining further accurate short-term WQP outcomes. The fundamental techniques of 2 hybrid techniques were XGBoost and RF that correspondingly present an innovative data denoising system - complete ensemble empirical mode decomposition with adaptive noise (CEEMDAN). Yan et al. [15] present a model to predict WQ dependent upon the DBN technique. Primary, the PSO technique was utilized for optimizing the network parameter of DBN which is for extracting the feature vector of the WQ time sequence dataset at several scales. Afterward, integrated with the least squares support vector regression (LSSVR) machine that is obtained as the predictive layer of models, a novel WQP approach mentioned that PSO-DBN-LSSVR is put forward.

This study explores the proposal of African Buffalo Optimization with the Deep Belief Network for Water Quality Prediction (PROPOSED) model in an IoT environment. The presented PROPOSED model majorly concentrates on the identification of water quality. To attain this, the PROPOSED model follows a two-stage process. At the initial stage, the DBN model analyses the water quality parameters to predict the WQI. In the second stage, the ABO algorithm is exploited as a hyperparameter optimizer to optimally modify the hyperparameters related to the DBN model which in turn enhances the classification outcomes. In order to discover the improved outcomes of the PROPOSED technique, a brief comparison study is performed.

## 2. The Proposed WQI Prediction Model

In this study, an effective PROPOSED methodology has been developed for the identification of water quality in the IoT environment. To attain this, the PROPOSED model follows a two-stage process, as discussed below.

### 2.1 Stage I: DBN-based Prediction

At the initial level, the DBN model analyses the water quality parameters to predict the WQI. The normalized dataset is subject to the classifier method. The presented method is described in the following: DBN is an intellectual methodology that involves different layers, whereby all the layers include visible neurons with the hidden and input layers with the output neuron [16]. As a result, the hidden layer made connections amongst input neurons; nonetheless, there is no linking between the hidden and the visible layers. The hidden and visible layer connection is regarded as exclusive and symmetric. For a provided input, the stochastic method recognizes the accurate output. The architecture  $St$  defines the pseudo temperature. The architecture of the stochastic model is determined by.

$$P_b(\zeta) = \frac{1}{1 + e^{-\frac{\zeta}{St}}} \quad (1)$$

$$F = \begin{cases} 1 & \text{with } 1 - P_b(\zeta) \\ 0 & \text{with } P_b(\zeta) \end{cases} \quad (2)$$

$$\lim_{St \rightarrow 0^+} P_b(\zeta) = \lim_{St \rightarrow 0^+} \frac{1}{1 + e^{-\frac{\zeta}{St}}} = \begin{cases} 0 & \text{for } \zeta < 0 \\ \frac{1}{2} & \text{for } \zeta = 0 \\ 1 & \text{for } \zeta > 0 \end{cases} \quad (3)$$

whereby a subset of RBM layers is positioned for extracting features and an MLP is applied. The energy of Boltzmann machines is arithmetically formulated for the binary state  $a$ , under the following equation, whereby  $w_{t_{x,y}}$  indicates the weights amongst  $\theta_i$  delineates the biases and the neurons.

$$\Delta E(a_x) = \sum_y a_x w_{t_{x,y}} + \theta_x \quad (4)$$

The energy definition of hidden and visible neuron joint composition  $(k, l)$  is represented in line with the following equations.  $k_x$  denotes the binary state of the hidden unit.  $b_x$  and  $c_x$  indicate the bias employed.

$$E(k, l) = \sum_{(x,y)} w_{t_{x,y}} k_x l_y - \sum_x b_x k_x - \sum_y c_y l_y \quad (5)$$

$$\Delta E(k_x, \rightarrow \vec{l}) = \sum_y w_{t_{xy}} l_y + b_x \quad (6)$$

$$\Delta E(\vec{k}, l_x) = \sum_y w_{t_{xy}} k_x + c_y \quad (7)$$

The input dataset likelihood distribution is encoded through the weight parameter allocated as the RBM learning pattern. The allocated probability is exploited through RBM training, in addition to the weight allotment described by the following equation.

$$Wt^{(g)} = \max_{Wt} \prod_{i \in K} p(\vec{k}) \quad (8)$$

For all the hidden and visible vectors, the adapted RBM method is specified where  $Y$  determines the partition function as follows.

$$p(\vec{k} \rightarrow l) = \frac{1}{S} e^{-E(\vec{k}, \vec{l})} \quad (9)$$

$$S = \sum_{\vec{k}, \vec{l}} e^{-E(\vec{k}, \vec{l})} \quad (10)$$

Since it is a difficult task to get the expectation sample over the dissemination described using the format, the learning method termed contrastive divergence (CD) is applied. Consequently, the summary of the CD approach is discussed below.

1. Select the trained sample  $k$  and brace in the visible neuron.
2. Decide the probability of hidden neuron  $p_l$ , by determining the weight matrix  $Wt$  and visible layer  $k$  products as  $p_l = \sigma(l \cdot Wt)$ , based on the following expression.

$$p(\vec{l}_y \rightarrow 1 | \vec{k}) = \sigma(c_y + \sum_x l_x w_{t_{x,y}}) \quad (11)$$

3. Examine the hidden state  $l$  from the probability  $p_l$ .
4. Describe the external products of vector  $k$  and  $p_l$ , and assumed as positive gradient  $\varphi^+ = k \cdot p_l^{st}$ .
5. Consider the reconstructed visible neuron  $k'$  from the hidden neuron  $l$ . Furthermore, it is necessary to confirm the hidden state  $l'$  from the visible neuron reconstruction  $a'$ .

$$p(\vec{k}_y \rightarrow 1 | \vec{l}) = \sigma(b_x + \sum_x k_y w_{t_{x,y}}) \quad (12)$$

6. Define the external product of  $k'$  and  $l'$ , and assumed a negative gradient  $\varphi^- = k' \cdot l'^{st}$ .
7. Find the upgraded weight using the following equation, in which  $\eta$  shows the learning rate.

$$\Delta Wt = \eta(\varphi^+ - \varphi^-) \quad (13)$$

8. The new value included in weight is upgraded according to the given formula.

$$wt'_{x,y} = \Delta wt_{x,y} + wt_{x,y} \quad (14)$$

Because of the learning procedure using the MLP method, consider the trainable pattern  $(J^g, O^g)$ , in which  $m$  defines the trained pattern count,  $1 \leq g \leq G$ ,  $J^g$ , and  $O^g$  indicates the input and desirable output vectors. As a result of the output neuron, every neuron error in  $y$  is described as follows. Therefore, the below equation provides the squared error of pattern  $m$  after the MSE as follows.

$$e_y^g = J^g - O^g \quad (15)$$

$$E_g^{mean} = \frac{1}{nh} \sum_{y=1}^h n (e_y^g)^2 = \frac{1}{nh} \sum_{y=1}^h n (J^g - O^g)^2 \quad (16)$$

$$E_{avg} = \frac{1}{G} E_g^{mean} \quad (17)$$

The DBN-trained model is the integration of normal training (MLP) and pretraining (RBM) is shown below.

1. Considering the arbitrarily chosen biases, weights, and other related variables, the DBN module is introduced.
2. The primary factor is an introduction of the RBM module using the input dataset which serves as the potential within the visible neuron and the unsupervised learning.
3. The input to the following layer is attained by a potential sample initiated in the hidden neuron of the early layer. Furthermore, it proceeds the unsupervised learning.

4. The process is sustained for a certain quantity of layers. As a result, the pretraining stage through RBM is determined till the attainment of MLP.

5. MLP step provides refined learning with the supervised form and is sustained till it accomplishes the targeted error rate. Fig. 1 demonstrates the infrastructure of the DBN technique.

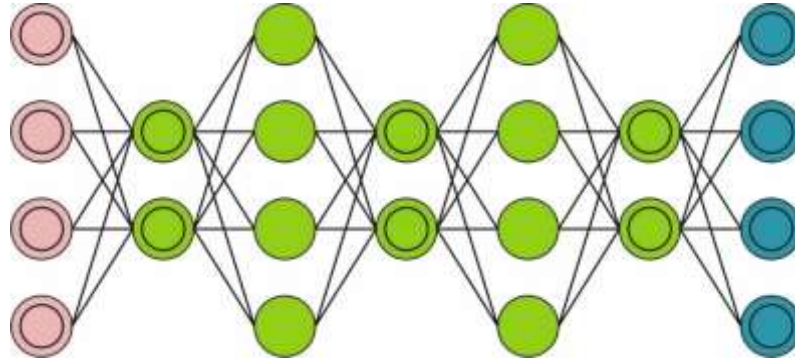


Figure 1: Architecture of DBN

## 2.2 Stage II: ABO-based Parameter Tuning

In this study, the ABO algorithm is exploited as a hyperparameter optimizer to optimally modify the hyperparameters related to the DBN model. Odili, Kahar, and Anwar [17] developed a simple, unique, and fast AFO technique for improving traveling salesman problems. The presented method is based on the movement of African buffalo that is herbivorous and migrates seeking lush green pasture. The herd of buffalo search for greenery and secure regions nearby South Africa. African buffalo have three notable characteristics that assist them in survival. The significant characteristic is that they intelligently interact with one another through the "waaa" and "maaa" sounds. "maaa" vocalization shows other buffalos in the herd that remain to utilize the current position since it is good and safe grazing pastures. "waaa" vocalization is a sign to other buffalos in the herd that keeps moving since the location is unsuitable or hazardous (attacks of other animals). The next characteristic is the wide memory capability to follow thousands of kilometers of paths. The foremost characteristic is the democratic behavior of buffalo. While conflicting calls in the herd by certain buffalo, the next "election" is considered by buffalo for taking the concluding decision to stay or move. This intelligent behavior of buffalo provides a large effective outcome. This behavior of buffalo to improve a decision tree (DT) is utilized in ABODT. In the study, an adapted form of ABO is utilized for creating better DTs that are optimized and efficient. The enhanced DTs provide good accuracy when compared to optimization algorithms and pruning of DTs.

The ABO technique initiates by randomly retaining every buffalo in an  $n$ -dimension solution space. In the study, the "waaa" signals represent exploration, and the "maaa" signal indicates exploitation of novel search. Afterward retaining buffalo in a random fashion, every buffalo exploitation (maaa" value)  $Ma_{k+1}$  is upgraded through  $bpr_{max}$  (optimal fitness of single buffalo) and  $bgr_{max}$  (optimal fitness of herd).

When the present fitness of buffalo is more efficient when compared to each maximal fitness ( $bgr_{max}$ ), and keep the position vector for certain buffalo. Once the current fitness is more efficient when compared to the herd's total optimal fitness, the herd's maximal fitness ( $bgr_{max}$ ) is stored and utilized in the following iteration. Each buffalo position is upgraded and look at the following buffalo [18]. Afterward checking global optimal fitness satisfies the existing condition, it stops the process and provides the stored presented potion as a solution to the problem. Once the optimal buffalo potion is not enhanced for iteration count, the entire herd is re-initiated and returns to step 2.  $lfrand_1$  and  $lfrand_2$  are learning parameters whose arbitrary value ranges from zero to one.

Because of the flexible behavior of the nature-inspired approach, adapted ABO is utilized for optimizing the DT. The resultant tree can able to perform global optimization. This simple, effective, and non-parameterized approach was never utilized beforehand in terms of DTs. The benefits of this adapted ABO technique are that it doesn't base on the parameter, is easier to implement, and is simplest to develop.

**Algorithm 1:** African Buffalo optimization (ABO)

1. Assume  $n$  buffalo with objective function  $f(x)x = (x_1, x_2, \dots \dots \dots x_n)^T$
2. Initialize buffalo: Place every buffalo in a random manner in the solution space.
3. for each  $k=1$  to  $n$  do  
(Continued on next page)  
Upgrade fitness value.  
 $Ma_{k+1} = Ma_k + lfrand_1(bgr_{max} - Wak) + lfrand_2(bpr_{max.k} - Wak)$
4. Upgrade the position of buffalo by about  $bgr_{max}$  and  $bpr_{max}$ .  
 $Wa_{k+1} = (Wa_k + Ma_k)/\pm 0.5$
5. Once  $bgr_{max}$  is Upgraded proceed to step 6 otherwise proceed to step 2.
6. Check for the ending condition, whether it satisfies, else process to step 3.  
end
7. Output optimal solution.

**3. Experimental Validation**

In this section, the experimental validation of the PROPOSED model is tested under distinct aspects. Table 1 and Fig. 2 provide a comparison of actual vs prediction outcomes of the PROPOSED model on pH values. The figure implied that the PROPOSED model has effectually predicted pH values under all iterations. For instance, with 25 iterations and an actual value of 0.007337, the PROPOSED model has a predicted pH of 0.003527. Next, with 50 iterations and an actual value of 0.012964, the PROPOSED method has a predicted pH of 0.004425. and then, with 75 iterations and an actual value of 0.012964, the PROPOSED approach has a predicted pH of 0.009424. At the same time, with 100 iterations and an actual value of -0.00839, the PROPOSED algorithm has predicted a pH of -0.00454.

Table 1: pH analysis of the PROPOSED approach with a distinct count of iterations

pH		
Iterations	Actual	Predicted
0	-0.00363	0.001121
25	0.007337	0.003527
50	0.003585	0.004425
75	0.012964	0.009424
100	-0.00839	-0.00454
125	0.004451	0.003161
150	0.018591	0.025771
175	0.000699	-0.0025

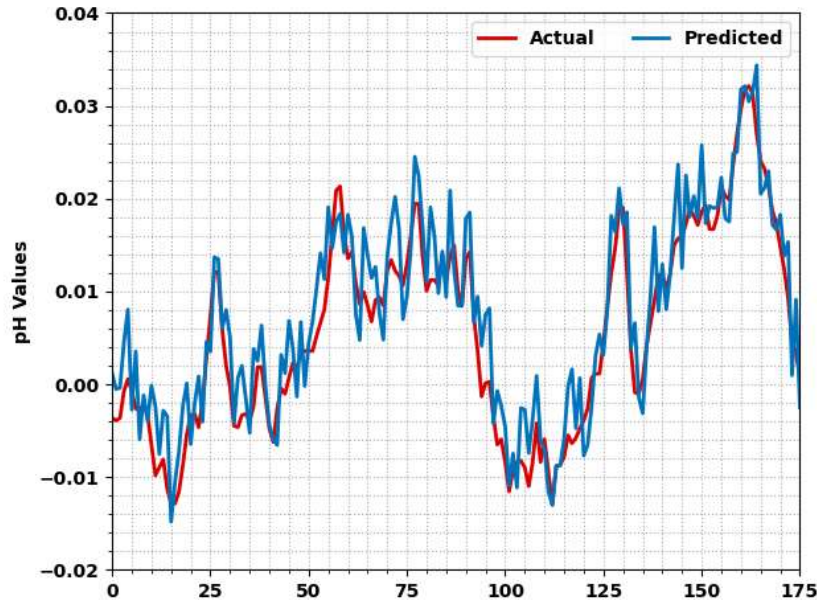


Figure 2: pH analysis of PROPOSED approach with a distinct count of iterations

Table 2 and Fig. 3 presents a comparative analysis of actual vs prediction outcomes of the PROPOSED technique on DO values. The figure implicit the PROPOSED approach has effectually predicted DO values under all iterations. For example, with 25 iterations and an actual value of 0.236775, the PROPOSED algorithm has predicted DO 0.219575. Subsequently, with 50 iterations and an actual value of -0.08751, the PROPOSED method has predicted DO -0.09551. Then, with 75 iterations and an actual value of -0.31642, the PROPOSED model has predicted DO -0.27722. Concurrently, with 100 iterations and an actual value of -0.16763, the PROPOSED technique has predicted DO -0.13313.

Table 2: DO analysis of the PROPOSED approach with a distinct count of iterations

Dissolved Oxygen (DO)		
Iterations	Actual	Predicted
0	0.164288	0.218088
25	0.236775	0.219575
50	-0.08751	-0.09551
75	-0.31642	-0.27722
100	-0.16763	-0.13313
125	-0.00548	0.025016
150	-0.14283	-0.14413
175	-0.22965	-0.23095

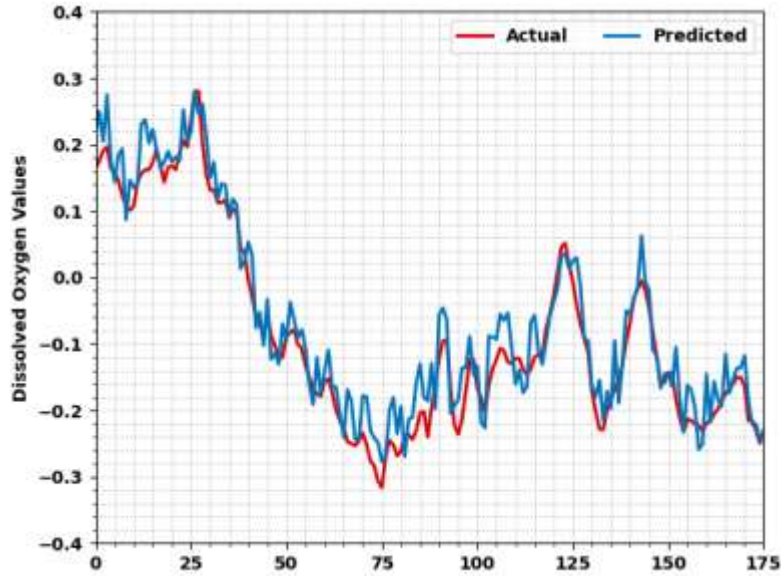


Figure 3: DO analysis of PROPOSED approach with a distinct count of iterations

Table 3 and Fig. 4 render a comparative study of actual vs prediction outcomes of the PROPOSED model on CON values. The figure implied that the PROPOSED model has effectually estimated CON values under all iterations. For example, with 25 iterations and an actual value of 0.022375, the PROPOSED model has estimated CON 0.006775. Then, with 50 iterations and an actual value of -0.05456, the PROPOSED model has predicted CON -0.02566. Also, with 75 iterations and an actual value of -0.01182, the PROPOSED model has predicted CON -0.01992. Finally, with 100 iterations and an actual value of -0.08448, the PROPOSED approach has predicted CON -0.09978.

Table 3: CON analysis of the PROPOSED approach with a distinct count of iterations

Conductivity (CON)		
Iterations	Actual	Predicted
0	0.013827	0.041727
25	0.022375	0.006775
50	-0.05456	-0.02566
75	-0.01182	-0.01992
100	-0.08448	-0.09978
125	0.07794	0.07664
150	0.381406	0.409906
175	-0.08675	-0.10395

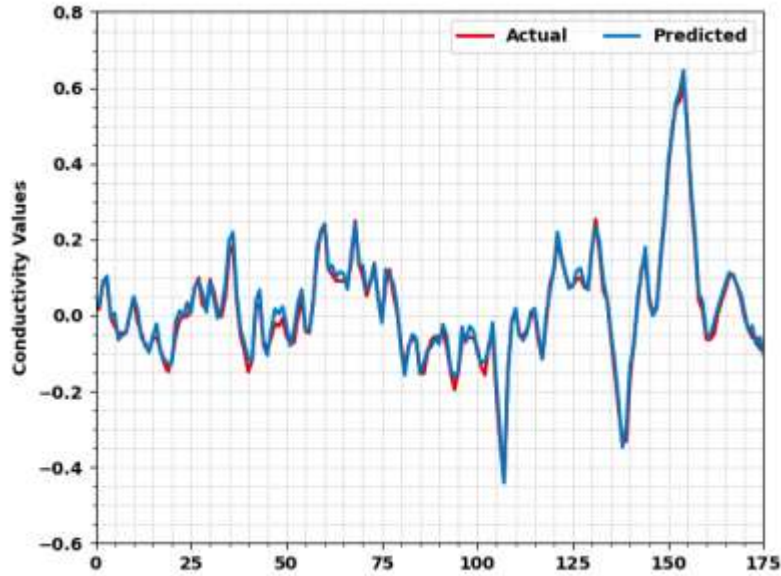


Figure 4: CON analysis of PROPOSED approach with a distinct count of iterations

Table 4 and Fig. 5 grant a comparative study of actual vs prediction outcomes of the PROPOSED method on TUR values. The figure implicit in the PROPOSED model has effectually predicted TUR values under all iterations. For example, with 25 iterations and an actual value of -0.19436, the PROPOSED model has predicted TUR -0.25796. Additionally, with 50 iterations and an actual value of -0.30761, the PROPOSED model has predicted TUR -0.22451. Besides, with 75 iterations and an actual value of 1.137956, the PROPOSED model has predicted TUR 1.127556. At last, with 100 iterations and an actual value of 0.478457, the PROPOSED model has predicted TUR 0.506557.

Table 4: TUR analysis of PROPOSED approach with a distinct count of iterations

Turbidity (TUR)		
Iterations	Actual	Predicted
0	0.058777	0.089677
25	-0.19436	-0.25796
50	-0.30761	-0.22451
75	1.137956	1.127556
100	0.478457	0.506557
125	0.132054	0.053954
150	-0.3609	-0.3762
175	0.215271	0.205571

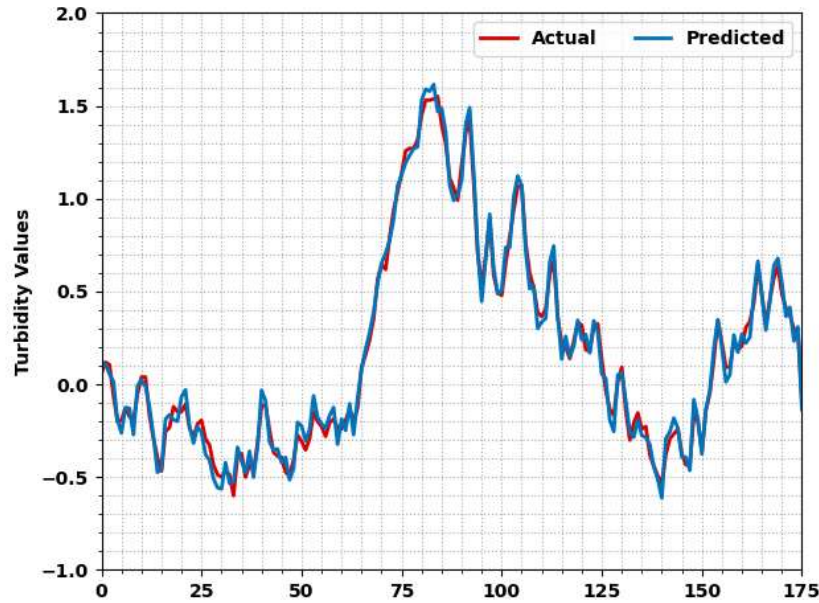


Figure 5: TUR analysis of PROPOSED approach with a distinct count of iterations

Table 5 and Fig. 6 presents a comparative analysis of actual vs prediction outcomes of the PROPOSED model on CODMn values. The figure denoted the PROPOSED model has effectually predicted CODMn values under all iterations. For example, with 25 iterations and an actual value of -0.10259, the PROPOSED model has predicted CODMn -0.13819. And then, with 50 iterations and an actual value of -0.17653, the PROPOSED model has predicted CODMn -0.11063. Next, with 75 iterations and an actual value of -0.737681, the PROPOSED model has predicted CODMn 0.715881. Further, with 100 iterations and an actual value of 0.025131, the PROPOSED approach has predicted COMn 0.013531.

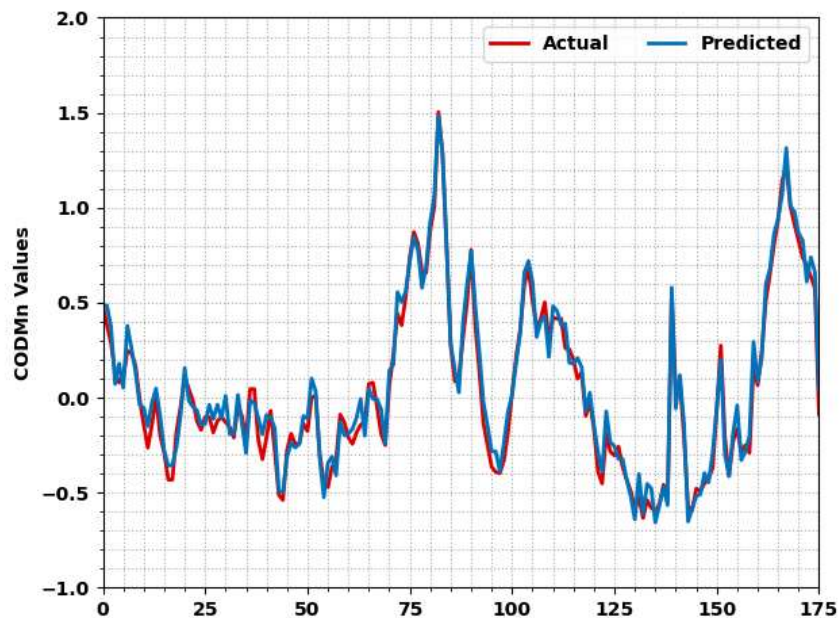


Figure 6: CODMn analysis of PROPOSED approach with a distinct count of iterations

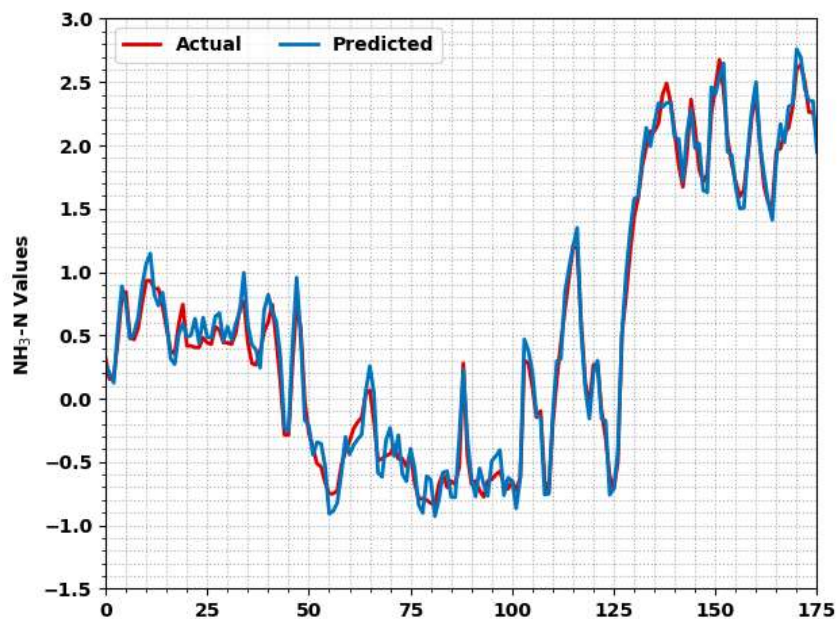
Table 5: CODMn analysis of PROPOSED approach with a distinct count of iterations

CODMn		
Iterations	Actual	Predicted
0	0.488961	0.482761
25	-0.10259	-0.13819
50	-0.17653	-0.11063
75	0.737681	0.715881
100	0.025131	0.013531
125	-0.30426	-0.25596
150	-0.06898	-0.05488
175	-0.04675	0.038847

Table 6 and Fig. 7 offer comparative scrutiny of actual vs prediction outcomes of the PROPOSED model on NH<sub>3</sub>-N values. The figure implied that the PROPOSED model has effectively predicted NH<sub>3</sub>-N values under all iterations. For example, with 25 iterations and an actual value of 0.441809, the PROPOSED model has predicted NH<sub>3</sub>-N 0.486009. Moreover, with 50 iterations and an actual value of -0.27392, the PROPOSED model has predicted NH<sub>3</sub>-N -0.21222. Also, with 75 iterations and an actual value of -0.4246, the PROPOSED model has estimated NH<sub>3</sub>-N -0.395. At last, with 100 iterations and an actual value of -0.65062, the PROPOSED model has predicted NH<sub>3</sub>-N -0.64852.

Table 6: NH<sub>3</sub>-N analysis of PROPOSED approach with a distinct count of iterations

NH <sub>3</sub> -N Values		
Iterations	Actual	Predicted
0	0.316242	0.272342
25	0.441809	0.486009
50	-0.27392	-0.21222
75	-0.4246	-0.395
100	-0.65062	-0.64852
125	-0.71341	-0.70991
150	2.463434	2.404534
175	2.074177	1.944477

Figure 7: NH<sub>3</sub>-N analysis of PROPOSED approach with a distinct count of iterations

Detailed WQI prediction results of the PROPOSED model are compared with recent models in Table 7 and Fig. 8. The experimental outcomes demonstrated that the ARIMA model has accomplished poor performance with a higher value of MSE. Then, the SVR and LSTM models reported slightly reduced MSE values of 0.005 and 0.002 respectively. Afterward, the PROPOSED model gained improved performance with the least MSE value of 0.001. Therefore, the PROPOSED model has shown improved forecasting outcomes over other models.

Table 7: MSE analysis of the PROPOSED approach with existing methodologies

Methods	MSE Values
ARIMA Model	0.025
SVR Technique	0.005
LSTMs Model	0.002
Ours	0.001

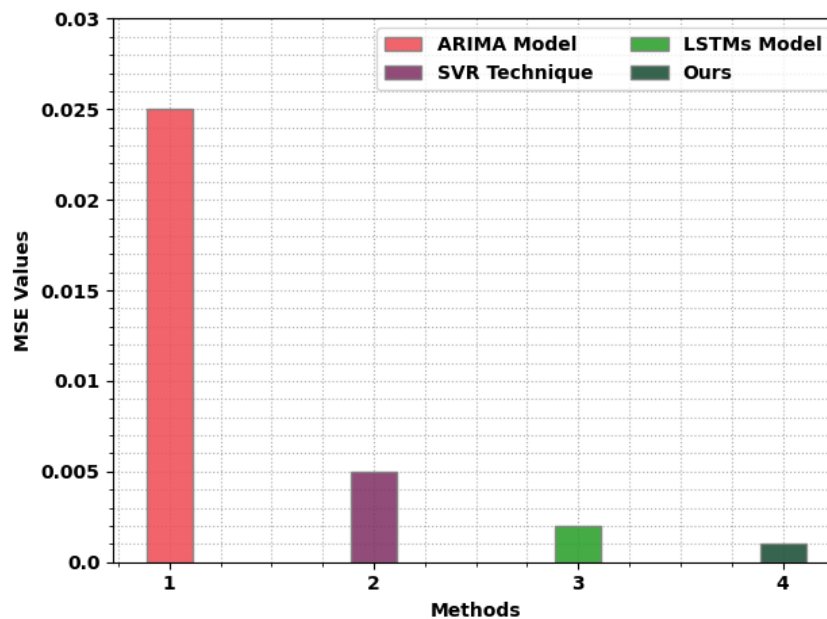


Figure 8: MSE analysis of the PROPOSED approach with existing methodologies

#### 4. Conclusion

In this study, an effective PROPOSED methodology has been developed for the identification of water quality in the IoT environment. To attain this, the PROPOSED model follows a two-stage process. At the initial stage, the DBN model analyses the water quality parameter to predict the WQI. In the second stage, the ABO algorithm is exploited as a hyperparameter optimizer to optimally modify the hyperparameters related to the DBN model which in turn enhances the classification outcomes. In order to discover the improved outcomes of the PROPOSED model, a brief comparison study is performed. The comparative outcomes reported the supremacy of the PROPOSED model over other approaches.

#### References

- [1] Bhutada, H., Khurshid, A., Yadav, M., Yadav, N. and Baheti, P., 2022, April. COD prediction in water using Edge Artificial Intelligence. In 2022 10th International Conference on Emerging Trends in Engineering and Technology-Signal and Information Processing (ICETET-SIP-22) (pp. 01-05). IEEE.
- [2] Liu, P., Wang, J., Sangaiah, A.K., Xie, Y. and Yin, X., 2019. Analysis and prediction of water quality using LSTM deep neural networks in IoT environment. Sustainability, 11(7), p.2058.
- [3] Rashid, M.M., Al-Akhir, N., Simi, S.A., Saha, J., Rahman, M.O. and Kibria, M.G., 2021. IoT based smart water quality prediction for biofloc aquaculture. International Journal of Advanced Computer Science and Applications, 12(6).

- [4] Barzegar, R., Aalami, M.T. and Adamowski, J., 2020. Short-term water quality variable prediction using a hybrid CNN–LSTM deep learning model. *Stochastic Environmental Research and Risk Assessment*, 34(2), pp.415-433.
- [5] Aggarwal, S., Gulati, R. and Bhushan, B., 2019, July. Monitoring of input and output water quality in treatment of urban waste water using IoT and artificial neural network. In *2019 2nd International Conference on Intelligent Computing, Instrumentation and Control Technologies (ICICT)* (Vol. 1, pp. 897-901). IEEE.
- [6] Mustafa, H.M., Mustapha, A., Hayder, G. and Salisu, A., 2021, January. Applications of IoT and Artificial Intelligence in Water Quality Monitoring and Prediction: A Review. In *2021 6th International Conference on Inventive Computation Technologies (ICICT)* (pp. 968-975). IEEE.
- [7] Cheng, L., Tan, X., Yao, D., Xu, W., Wu, H. and Chen, Y., 2021. A fishery water quality monitoring and prediction evaluation system for floating UAV based on time series. *Sensors*, 21(13), p.4451.
- [8] Yang, Y., Xiong, Q., Wu, C., Zou, Q., Yu, Y., Yi, H. and Gao, M., 2021. A study on water quality prediction by a hybrid CNN-LSTM model with attention mechanism. *Environmental Science and Pollution Research*, 28(39), pp.55129-55139.
- [9] Li, Z., Peng, F., Niu, B., Li, G., Wu, J. and Miao, Z., 2018. Water quality prediction model combining sparse auto-encoder and LSTM network. *IFAC-PapersOnLine*, 51(17), pp.831-836.
- [10] Baek, S.S., Pyo, J. and Chun, J.A., 2020. Prediction of water level and water quality using a CNN-LSTM combined deep learning approach. *Water*, 12(12), p.3399.
- [11] Zou, Q., Xiong, Q., Li, Q., Yi, H., Yu, Y. and Wu, C., 2020. A water quality prediction method based on the multi-time scale bidirectional long short-term memory network. *Environmental Science and Pollution Research*, 27(14), pp.16853-16864.
- [12] Yan, J., Liu, J., Yu, Y. and Xu, H., 2021. Water quality prediction in the luan river based on 1-DRCNN and bigru hybrid neural network model. *Water*, 13(9), p.1273.
- [13] Aldhyani, T.H., Al-Yaari, M., Alkahtani, H. and Maashi, M., 2020. Water quality prediction using artificial intelligence algorithms. *Applied Bionics and Biomechanics*, 2020
- [14] Lu, H. and Ma, X., 2020. Hybrid decision tree-based machine learning models for short-term water quality prediction. *Chemosphere*, 249, p.126169
- [15] Yan, J., Gao, Y., Yu, Y., Xu, H. and Xu, Z., 2020. A prediction model based on deep belief network and least squares SVR applied to cross-section water quality. *Water*, 12(7), p.1929
- [16] Liu, S., Xie, J., Shen, C., Shang, X., Wang, D. and Zhu, Z., 2020. Bearing fault diagnosis based on improved convolutional deep belief network. *Applied Sciences*, 10(18), p.6359.
- [17] Odili, J.B., Kahar, M.N.M. and Anwar, S., 2015. African buffalo optimization: a swarm-intelligence technique. *Procedia Computer Science*, 76, pp.443-448.
- [18] Singh, P., Meena, N.K., Slowik, A. and Bishnoi, S.K., 2020. Modified african buffalo optimization for strategic integration of battery energy storage in distribution networks. *IEEE Access*, 8, pp.14289-14301.